Enhancing Wireless Performance Using Reflectors

Sihui Han and Kang G. Shin
Department of Electrical Engineering and Computer Science
The University of Michigan
Ann Arbor, MI 48109-2121
Email: {sihuihan,kgshin}@umich.edu

ABSTRACT

Signal decay is the fundamental problem of wireless communications, especially in an indoor environment where line-of-sight (LOS) paths for signal propagation are often blocked and various indoor objects exacerbate signal fading. There are three reasons for signal decay: long transmission distance, signal penetration and reflection. In this paper, we propose `OptRe` which optimally places metallic reflectors — providing a highly reflective surface that can reflect impinging signals almost 100% — in indoor environments to reduce the reflection loss and enhance wireless transmissions. It enhances both WiFi signal and low-power IoT devices without changing their configurations or network protocols. To enable `OptRe`, we first develop an empirical signal propagation model that can accurately estimate the signal strength and adapt itself to the reflectors' location. Using micro-benchmarks, our empirical signal propagation model is shown to be more accurate than the other existing path loss models. We also optimally place reflectors to maximize the worst-case signal coverage within the target indoor areas. Our extensive experimental evaluation results have shown `OptRe` to enhance signal strength for different types of wireless signals by almost 2x.

1. INTRODUCTION

Significant efforts have been made to mitigate the fading of wireless signals, including WiFi, BLE and ZigBee signals used by low-energy IoT devices. A simple way is to add more Txs to cover blind or weak-signal areas. However, it not only increases the cost of deployment, but also incurs additional interferences which are even more difficult to handle. Increasing the transmission power can also compensate for the signal's energy loss, but it is upper-bouded, typically by maximum effective isotropic radiated power (EIRP) set to 36dBm for WiFi according to the FCC regulation [1]. Even worse, most IoT devices use Bluetooth Low Energy (BLE), in which the transmission power is limited to $7\sim10$ dBm [2]. Other advanced techniques such as OFDM [3] and beamforming in MIMO systems [4] can enhance network performance, but they are only available on the newest WiFi devices and cannot be applied to low-power IoT devices with only limited signal processing resources.

All of the above-mentioned schemes focus on the two ends of the Tx–Rx path, not the signal decay along the propagation path in between, limiting their ability to reduce signal decay. The fundamental challenge in mitigating the signal decay comes from the complexity of real-life indoor environments due mainly to the existence of various indoor obstructions, blocking the line-of-sight (LOS) path between Tx and Rx, and generating complicated multipath effects. Such complexity invalidates most of the existing models such as Rayleigh fading model [5], and makes it difficult to accurately model the transmission environment. Even with the path loss model that can characterize the signal propagation, how to apply the model is still an open problem.

In this paper, we propose use of metallic plates (mainly aluminum plates) as reflectors which can reflect the wireless signals to reduce the signal fading during reflections. The reflectors do not focus light, and hence won't annoy people in the building. We make the following main contributions:

- Design of `OptRe` to enhance wireless network performance by optimally placing reflectors without requiring advanced signal processing in wireless devices.
- Design of a novel empirical signal propagation model which can be adapted to the change of reflector locations, and training of the model parameters using the simulated annealing.
- Proposal of a greedy reflector placement algorithm which is the first of its kind to maximize the worst coverage performance within the target area by changing the reflector's location for both WiFi and IoT devices.
- Demonstration of two use-cases of `OptRe`: enhancing coverage and connectivity of low-power IoT devices and customizing AP coverage for security.

The rest of the paper is organized as follows. Section 2 motivates the design of `OptRe`. Section 3 details the overall system and functionalities of `OptRe`. We evaluate the performance of `OptRe` in Section 4 and discuss two prominent use-cases of `OptRe` in Section 5. The remaining issues are discussed in Section 6. After reviewing the related work in Section 7, we finally conclude the paper in Section 8.

2. WHY REFLECTORS?

Without relying on use of advanced signal processing at Tx/Rx sides and by only utilizing cheap metal plates as reflectors, `OptRe` can both enhance the signal strength by preventing signal absorption during its reflection, and block the signal from penetrating through the reflectors. How could

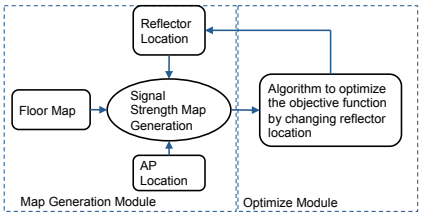

Figure 1: System overview.

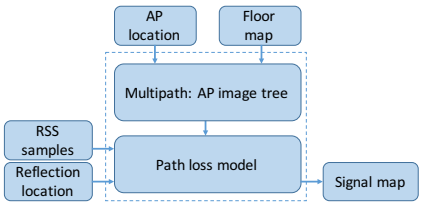

Figure 2: Map-generation module.

such functionalities of OptRe improve our daily lives? Given below are two proof-of-concept use-cases of OptRe that enhance the performances of wireless devices.

Enhance coverage and connectivity for WiFi and IoTs. These become a more challenging problem for low-power IoT devices due to limited processing resources and their transmission range is only a few meters. For example, after a smartwatch is paired with a smartphone using Bluetooth, if the user moves from the study room to the kitchen without his smartphone, the smartwatch might lose connection to the smartphone and can't access the Internet. The same applies to the connection between IoT devices and the IoT gateway which is restricted to cover a small region. OptRe provides the functionalities required for improving coverage and connectivity with fixed transmission power for both WiFi and IoTs without modifying the device configuration, by eliminating the signal reflection loss along the propagation paths. It can also lower the transmission power to ensure the same transmission range, further reducing the power of IoTs when they are close to the IoT gateway and extend their lifetime. Note that reflectors benefit both uplink and downlink transmissions, since both use the same signal propagation path.

Customize the signal propagation for security and privacy. Wireless transmissions are vulnerable to traffic eavesdropping and other security and privacy attacks. Malicious users in a region where the signal strength is sufficiently strong, can eavesdrop data transmission. Even if the wireless network is encrypted, they can still obtain network information (e.g., channel number, received signal strength), and use the information to physically locate the AP or launch Denial-of-Service (DoS) attacks. The functionality of OptRe, which avoids signal penetration by near perfect reflection, provides an effective way to avoid eavesdropping, and complements other existing defense mechanisms. We can intelligently control the signal strength in target regions using reflectors where third-parties may eavesdrop.

3. SYSTEM DESIGN

We want to place reflectors "optimally" and adaptively to different indoor environments. We will first overview OptRe and then detail its design.

3.1 System Overview

OptRe consists of two main modules, map-generation and optimization, as shown in Fig. 1.

Map-Generation Module: This module takes floor map, AP location and current reflectors' locations as input, and outputs the corresponding RSS estimation within the target area (i.e., an RSS signal map). The thus-obtained signal map will be fed to the optimization module so as to determine the optimal locations of reflectors.

Optimization Module: This module takes the RSS signal map from the map-generation module as input and uses heuristics to determine the updated reflector locations. It then feeds the new locations to the map-generation module to get the updated RSS estimation. These two modules execute alternately to get the reflector locations.

3.2 Map-Generation Module

Indoor radio propagation has been an active subject of research [6, 7]. A detailed description of earlier radio propagation models can be found in [8]. The representative models range from a simple uniform path-loss model [9] to sophisticated models such as empirical models for indoor signal propagation (ITU model [10]) and ray-tracing models [11]. All of these have several shortcomings: (1) tedious measurements are required to determine the building-specific attenuation exponent and coefficients of indoor partitions; (2) detailed material characteristics and geometry properties are required if a site-specific model is to be used; (3) re-measurements are needed in case of environmental changes (including the reflection/penetration changes caused for any reason).

It is impractical to use the existing empirical path-loss models which require re-measurements whenever the reflector location changes. So, we propose a new model which requires neither information on object material and AP configuration nor re-measurements. Specifically, we (i) model the multipath transmission of WiFi signals and (ii) acquire the received signal strength (RSS) using our path-loss model, as shown in Fig. 2.

3.2.1 Multipath reflection pattern of WiFi signals.

Wireless signals reach the receiving antenna via multipaths due to reflection, refraction, etc. Ray-tracing is a common way to characterize the multipaths to Rx, which is based on the fact that the wireless signal is an electromagnetic wave following the reflection law. It tracks the images of Tx by objects such as walls and furniture to obtain each ray (transmission path). Fig. 3 shows a simple case — a rectangle area with four walls and one Tx/Rx pair — and two rays that first go through the upper wall as an example. In Fig. 3, point (1,1) represents the image of Tx by the upper wall, and (2,1), (2,2), and (2,3) are the images of (1,1) by left, right, and under walls, respectively. By connecting Tx,

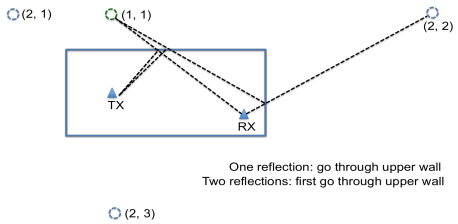

Figure 3: Radio propagation with ray tracing.

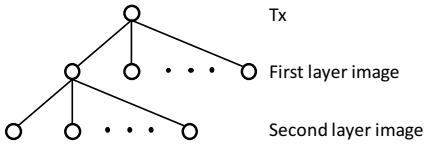

Figure 4: Image recording tree.

reflection point, and Rx, we can get a ray from Tx to Rx. There could be many rays reaching Rx after multiple reflections. Since wireless signals decay during their transmission, only the rays that have enough power and experience a limited number of reflections contribute to the received signal. So, we only need to consider a limited number of reflections and rays. For efficient management of the reflection map, we introduce an Image Recording Tree (IRT) as shown in Fig. 4, which contains the metadata of multipath rays. The root of the IRT is the Tx, and the first level of the tree stores the information of Tx images (including coordinates and information of the wall it is located at). The children of each node is the image of their parents over each of the walls. The leaf nodes are the reflection points closest to Rx. By connecting Rx and a leaf node and then traversing up along the parent node to the root, we can get a single ray which arrives at Rx from Tx following the reverse route. The depth of the IRT represents the maximum number of reflections we need to consider. Fig. 4 shows the case of considering at most two reflections in each ray which can be adjusted depending on the use-case. We can prune the tree further based on the restriction that the reflection point should lie within the wall range. Using IRT, we can derive the propagation path from Tx to a specific Rx location, including the number of rays and reflections, reflection point, and reflection angle of each ray. The remaining problem is then how to characterize the path loss for each ray based on its reflection features, and then estimate the RSS at Rx.

3.2.2 Empirical Path-Loss Model

The signal power at Rx is the accumulated power of all individual rays from the same Tx. The path loss of each ray includes the distance-dependent loss and attenuation due to reflections. As in [12, 13], we focus on modeling the average of RSS over time, and ignore the phase differences among rays which are usually used to study the variance of RSS over time. The model is then defined as:

$$P = P(LOS) + \sum_{i=1}^{n^t-1} P_i, \tag{1}$$

where P is the power at Rx, n_t is the total number of received

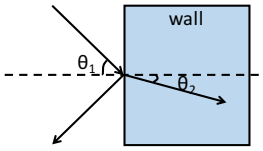

Figure 5: Illustration of reflection and refraction.

rays obtained from IRT; $P(LOS)$ is the RSS of LOS which can be easily calculated by using the free-space path-loss model and P_i is the power of the i^{th} reflected ray. The signal power of each reflected ray can be derived as:

$$P_i = P(LOS_1)\prod_{j=1}^{m_i}(R_j P(LOS_{j+1})), \tag{2}$$

where m_i is the number of reflections of the i^{th} ray (that can be obtained from IRT), and R_j is the reflection coefficient of the i^{th} reflection. $P(LOS_{j+1})$ is the path loss of the $(j+1)^{th}$ LOS (e.g., a two-reflection ray path consists of three parts of LOS transmissions intersected at the reflection points as shown in Fig. 3). $P(LOS_j)$ denotes only direct transmission without reflection, different from the free-space model.

The reflection coefficient varies with the materials, and equals 1 for metal reflectors. Considering the walls and other objects as homogeneous dielectric slabs, and assuming parallel polarization [14], the reflection coefficient R is:

$$R = \frac{\eta_1 cos\theta_1 - \eta_2 cos\theta_2}{\eta_1 cos\theta_1 + \eta_2 cos\theta_2}, \tag{3}$$

where η_1, η_2 are wave impedances, and θ_1 and θ_2 are incidence and refraction angles as shown in Fig. 5. By Snell's law [15] θ_2 is related to θ_1 via $\sqrt{\varepsilon_2}sin\theta_2 = \sqrt{\varepsilon_1}sin\theta_1$, where ε_1 and ε_2 represent material permittivity. Combining this with Eq. (3), R is:

$$R = \frac{\frac{\alpha}{\sqrt{1-\beta sin^2\theta_1}}cos\theta_1 - 1}{\frac{\alpha}{\sqrt{1-\beta sin^2\theta_1}}cos\theta_1 + 1}, \tag{4}$$

where α and β are the parameters that need to be tuned empirically and θ_1 can be obtained from IRT.

So far, we have modeled the reflection path loss (Eq. (1)) and the only unknown parameters are α and β which can be obtained from measurements. Since α and β will not vary with the reflector location, the above path-loss model can be utilized to estimate RSS for reflector placement.

To incorporate the penetration effect, we slightly modify the free-space model [16] and define $P(LOS_j)$ in Eq. (2) as $P(LOS_i) = \frac{\gamma^p \delta}{d_i^2}$, where $\delta = (4\pi)^2 G_R P_T G_T$ is the free-space model parameter that depends only on Tx and Rx; P_T, G_T, and G_R denote transmission power, Tx and Rx antenna gains, respectively. λ represents the signal wavelength and d is the distance between Tx and Rx. γ represents the penetration coefficient, and p the penetration delays occurred along the path. Note $p = 1$ when there is no penetration and $P(LOS_i)$ thus degenerates to the free-space model.

Thus far, we have demonstrated our signal propagation model: α and β are used to model the reflection; penetration

can be characterized by γ, and δ represents the characteristics of Txs and Rxs. Note that our model uses single α, β, γ to generalize the characteristics of all the objects (including walls, doors and furnitures) and we will collect real data from measurements to obtain its proper values.

3.2.3 Training α, β, γ, δ in Path-Loss Model

It requires measurements at reference locations to estimate these parameters. If a maximum of n reference measurements are available, a linear system of $Ax = b$ (derived from Eq. 2) can be used to determine the unknowns $x = [\alpha, \beta, \gamma, \delta]^T$. To solve the linear equations, the method of least squares could be used. From the ray tracing simulation, there exist a maximum number of N rays, but only $n < N$ rays are actually received because of the different attenuation along each individual path. Since some rays are too weak to contribute the energy at Rx, we exclude them from the linear system. Such an elimination process is difficult to do at this stage because of lack of energy information. We use simulated annealing (SA), a randomized algorithm, to search for the optimal values of $x = [\alpha, \beta, \gamma, \delta]^T$ that minimize the mean square error (MSE) of the RSS estimation. To calibrate these parameters, we only need measurements at a small number of sampled locations, rather than a complete site survey. Thus, our model can be easily adapted to different environments.

Simulated Annealing (SA) Algorithm:

SA is used to search for the optimal solution based on the way that a metal cools down to the optimal state (the annealing process from an initial temperature T to minimal T_{min} at a certain cooling rate) [17]. Algorithm 1 keeps on running (cooling) until T reaches T_{min}, and examines a candidate solution for each T. It not only accepts candidate solutions which are strictly better than the previous one ($MSE' < MSE$), but also accepts a worse fitness candidate with an acceptance probability $p \leftarrow e^{\frac{MSE'-MSE}{T}}$ to avoid getting stuck at local minima. The algorithm gets more conservative as T decreases, and converges to the global optimum. The algorithm calls *upDateMdl()* to yield a solution near the current solution *mdl* (next candidate solution). It alters α, β, γ and δ by Δ, where Δ is uniformly distributed within $[-\frac{p}{10}, \frac{p}{10}]$, and p represents the parameter being updated.

SA trains the parameter within 100*ms*, and the map-generation module outputs the estimated signal map within 300*ms* for a $7m \times 9m$ residential environment and 2*s* for a $10m \times 30m$ office environment. While we use the 2D propagation model (since 2D floor maps are easy to obtain), `OptRe` is general and is easily extensible to the 3D space by incorporating the signal's interaction in the 3D environment.

To validate the map-generation module, we conducted experiments in both residential and office environments (Section 4.2). The model can accurately estimate the signal map which can be used to optimize the reflector placement.

3.3 Optimization Module

Algorithm 1 Simulated Annealing for Tuning Model

```
T ← 1000
T_min ← 0.001
coolingRate ← 0.999
Initialize model parameter mdl(α, β, γ, δ)
RSS_pred ← getSingalMap(IRTree, mdl)
MSE ← getMSE(RSS_gnd, RSS_pred)
while T > T_min do
    mdl' ← upDateMdl(mdl)
    RSS_pred ← getSingalMap(IRTree, mdl')
    MSE' ← getMSE(RSS_gnd, RSS_pred)
    p ← e^((MSE'−MSE)/T)
    if MSE' ≤ MSE or rand[0,1] ≤ p then
        MSE ← MSE'
        mdl' ← mdl
    end if
    T ← T · coolingRate
end while
mdl* ← mdl
End
```

Given the path-loss model and the AP's location, the problem of optimal placement of reflectors is transformed to that of maximizing the network performance in a given area.

3.3.1 Objective function

To ensure acceptable performance at the worst Rx location (with minimum RSS), we consider use of the max min objective function. Let $P_i(Loc_r)$ be the signal strength at the i^{th} Rx location when the reflector is placed at Loc_r, then the objective function is defined as:

$$\textbf{P: } \max\min\ P_i(Loc_r), \quad \forall i \in m \tag{5}$$

where m is the number of Rx locations we consider, w_i the weight (priority) for the i^{th} Rx's location, and g_I the minimal signal strength requirement for all Rx locations. Note that the above objective function is to improve the coverage at the worst Rx location, and the worst RX location can be easily determined by the map-generation module.

The objective function relies on the signal strength estimation from the path-loss model which is neither continuous nor expressable in closed form, so it is difficult to apply the existing optimization tools. To address this problem, we apply a greedy algorithm to derive the optimal reflector locations. Without loss of generality, we assume the size of reflector is fixed and aim to find the optimal location for k reflectors placed on the walls. For a 2D floor map, the reflectors will be represented as lines with unit length.

3.3.2 Greedy Algorithm

We apply a greedy algorithm to solve the problem approximately instead of trying to find the optimal solution. The greedy algorithm selects the top k reflector locations which individually yield top k improvements in our objective func-

Algorithm 2 Greedy Reflector Placement

```
Precompute all candidate reflector locations: {RL}.
Reflector locations: {Loc_i, i ∈ k}
Top objective function values: {Obj_i, i ∈ k}
for rl : RL do
    cur ← calcObj(rl, mdl)
    if cur > min(Obj_i, ∀i ∈ k)) then
        Update {Obj}, {LOC}
    end if
end for
Return {LOC_i, ∀i ∈ k}
End
```

tion. As shown in Algorithm 2, we first need to enumerate all the candidate reflector locations, which basically cover all the walls in the targeted area. We then iterate through all the candidates and get the top k locations which have the largest objective function, using the Quickselect algorithm [18]. The objective function improves the worst-case performance in the targeted area.

The number of reflectors depends on the layout of the target area. The greedy algorithm in the optimization module selects the top k reflector locations that improve the worst-case RSS to the largest extent. The exact value of k depends on the building layout and can be derived by the greedy algorithm (based on the performance difference of using k and $k+1$ reflectors). As k increases, the improvement converges to a stable stage. Since reflectors can only reduce the reflection loss during signal penetration and cannot reduce the penetration and distance loss, the RSS will be bounded by the penetration loss and distance loss, and can't keep on increasing after enough reflectors are placed.

4. EVALUATION

4.1 Testbed Setting

We first evaluate the accuracy of map-generation module using off-the-shelf Wi-Fi NICs. Then, to evaluate the optimization module, we build a software-radio testbed with WARP boards [19] configured as WiFi Tx/Rx using 802.11a standard reference design (as shown in Fig. 6(a)).

We conducted experiments in both home and office environments: (i) a one-bedroom apartment and (ii) an office building. In the home environment, the AP was placed at the corner (A) and center (B) of the living room, shown as blue triangles in Fig. 6(b). The office environment is depicted in Fig. 6(c). There are 3 orange-colored areas of which area A is chosen as our target to validate the map-generation module. We also evaluate the optimization module in the office environment: we start with area A in Fig. 6(c) and then extend the result to all the three target areas.

4.2 Empirical Validation of Path-Loss Model

We built a detailed to evaluate the accuracy of map-generation module. The simulator applies the path-loss model in Section 3 and tunes the parameters using the SA algorithm as shown in Section 3.

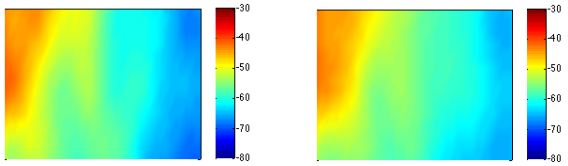

(a) Measured signal map (b) Estimated signal map

Figure 9: Signal map in the office environment.

Our Wi-Fi Tx is an ASUS RT-AC66U wireless router with 2 external antennas operating on 2.4/5GHz dual-band. The router's operating channel is set to the least congested channel to minimize interference from other Wi-Fi links. The receiver is a MacBook Pro. The space under consideration is partitioned into 1m$\times$1m grids. For baseline measurements without reflectors, we place the receiver at the center of each cell, capture the router's beacons for 60 seconds using WireShark, and average the RSS values.

To obtain α, β, γ δ, we applied 6 of the 44 measured baseline RSSs as training samples to tune the model. Note that the training points should span the whole area and also include the points close to the walls to capture the effects of the walls on reflection and penetration.

4.2.1 Home Environment

The size of apartment we considered is 6.4m$\times$ 9.14m, and the measured/estimated RSSs are plotted as signal maps. Fig. 7(a) shows the baseline signal map where the AP is at location A (at the corner of the living room), and the estimated signal map is shown in Fig. 7(b). The signal, as shown in Fig. 7(a), not only decays as the distance from Tx increases, but also has irregular fluctuations due to multipaths of reflections and penetrations. To validate the model in different scenarios, we move the AP to the center of the living room (location B). The corresponding baseline and estimated signal map are shown in Figs. 7(c) and (e), yielding a similar pattern. Comparing the baseline signal map between the case where AP is at the corner and at the center (Fig. 7(a) and (d)), one can see the signal strength surrounding the AP much stronger when the AP is at the corner near the walls. Despite the reflection loss by the surrounding wall, the partial signal after reflection still contributes to RSS.

We compare `OptRe` with the widely used propagation models: (i) log-distance path loss model [9], and (ii) site-specific ITU indoor path loss model [10]. To quantify the performance, we analyze the CDF of the L1-norm error of the estimated RSS. Figs. 8(a) and (b) show the results when the AP is at the corner and center, respectively. The error of `OptRe` is no more than 5dBm and less than 3dBm with a probability of about 0.8. The log-distance model only focuses on distance loss without considering the effect of reflection and penetration. Thus the error is up to 15dBm (Fig. 8(a)). ITU considers the site-specific parame-

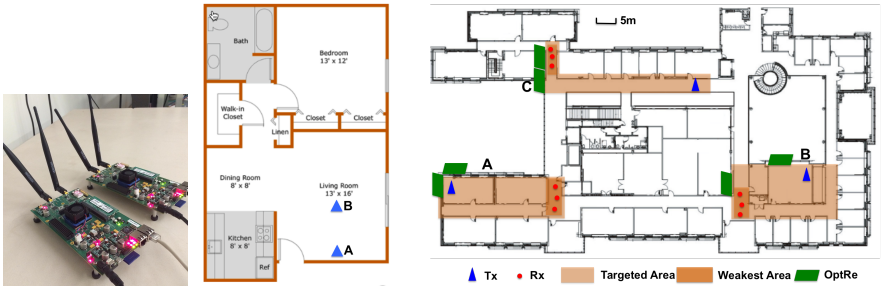

(a) (b) (c)

Figure 6: Test environments: (a) WARP boards, (b) home environment: 1-bedroom apartment (for validation of map-generation module), (c) office environment: 4th floor of our Department building (for validation of both modules of `OptRe`).

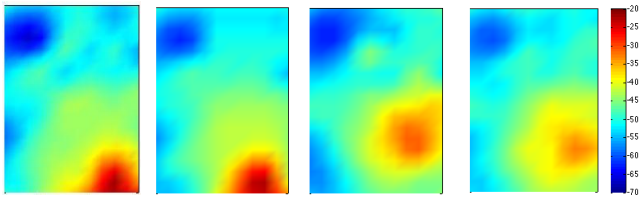

(a) (b) (c) (d)

Figure 7: Signal propagation map in the home environment: (a) measured signal map with AP at the corner of the living room, (b) estimated signal map with AP at the corner, (c) measured signal map with AP at the center of the living room, (d) estimated signal map with AP at the center.

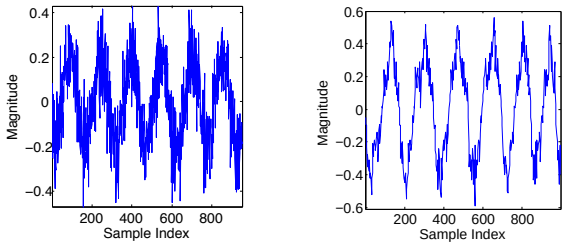

(a) w/o reflector (b) w/ reflector at Rx side

Figure 10: Performance of reflector in time domain.

ters while requiring detailed material characteristics and geometry properties. No detailed information is available, so ITU performs even worse than the log-distance model. In summary, `OptRe` reduces the estimation error by about 50% over the log-distance and ITU path-loss models regardless of the AP's location.

4.2.2 *Office Environment*

Our model is also validated in an office environment as shown in Fig. 6(c), while focusing on area *A*, the bottom left orange shaded area (around 8m ×24m). Following the same procedure as in the home environment, we measure the baseline signal map and estimate the signal map as shown in Fig. 9 and the CDF of the estimation error as shown in Fig. 8(c). The error is no more than 4dB and less than 2dB with over 50%. Therefore, the map generation is shown to be accurate in both home and office environments.

4.3 Performance of `OptRe`

Using the map-generation module, we can easily locate the worst coverage area (i.e., the lowest RSS), and then use `OptRe` to enhance the worst-case performance. We implemented 802.11a standard on 2 WARP boards [19] and set the transmission power to the default value, 30dBm.

In our test environment, two reflectors ($k = 2$) are placed according to the greedy algorithm's result. We start with area *A* in Fig. 6(c). The Rx WARP board can be anywhere within the orange-colored subarea in *A*. The weakest signal regions are shown in dark orange, where 3 Rx locations are uniformly and randomly selected (red circles in Fig. 6(c)). The green parallelograms in Fig. 6(c) are the reflector locations determined by `OptRe`. At each Rx location, we ran experiments for 100s and averaged the results.

We evaluate the received signal in time and frequency domains, and the effect of `OptRe` on RSS, SINR and data rate. All the following results represent the worst case within the target area (orange-colored zone). The worst-case improvement guarantees that the users (including mobile users) would not enter a "blind" zone and prevents the extreme cases like loss of connection.

4.3.1 *Impact of* `OptRe` *in Time Domain*

We start with the time domain analysis and measure the magnitude of the signal. Figs. 10(a) and (b) show the amplitude of the received signal without reflectors and with `OptRe`, respectively. `OptRe` reduces the reflection loss during transmission, and hence improves the amplitude of the received signal by about 40% and smooths the signal with less jitters. To further analyze the reason for less jitter in the time domain after placing reflectors, next we study the signal in the frequency domain.

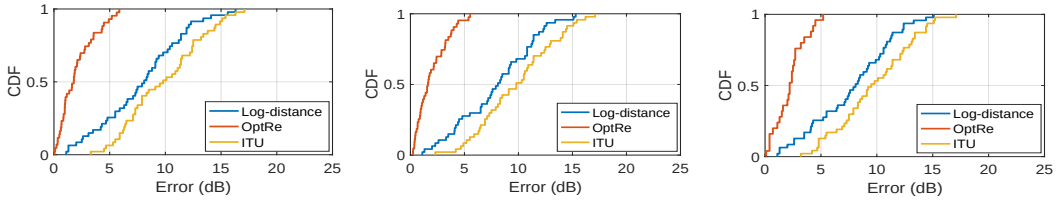

(a) Home environment (b) Home environment (c) Office environment

Figure 8: CDF of estimation errors: (a) AP at the corner, (b) AP at the center, (c) the office environment.

4.3.2 *Impact of* `OptRe` *in Frequency Domain*

OFDM [3] is widely used in wireless communications: orthogonal subcarrier signals (usually 64 subcarriers in 20MHz bandwidth) are used to carry data on parallel data streams. We measured the signal attenuation on each subcarrier for 60 times. Fig. 11 shows the SNR of received signal with and without `OptRe`, and different colors represent different trials. The SNR varies due to selective frequency fading [20]. The peak SNR without reflectors is 12dB, and over 60% of the SNR is below 8dB. As shown in Fig. 11(b), the maximum SNR is improved by 25% and rises up to 15dB after using `OptRe`. More than 80% of the SNR in all frequencies is above 8dB. `OptRe` improves SNR on different frequencies and reduces the frequency selective fading, making the signal pattern in time domain less jittery and easy to decode.

4.3.3 *Impact of* `OptRe` *on RSS & SINR*

We compare the performance in three cases: (i) without reflectors; (ii) placing reflectors near worst-case locations; (iii) placing reflectors by `OptRe`. Placing reflectors near worst-case locations is an intuitive method which can bounce and accumulate signals. We consider it as an alternative baseline and will henceforth call it "placing at Rx side".

Figs. 12 (a) and (b) show the RSS and SINR performance, respectively. Without using reflectors, the smallest RSS within the targeted area A is around -81dBm and SINR is around 5dB. After placing reflectors at Rx-side, RSS increases to -78dbm and SINR to 7dB. With `OptRe`, the RSS and SINR are improved to -75dBm and 9dB, respectively, which is 50% better than the Rx-side scheme. 3dB difference in SINR typically leads to one modulation level improvement [21]. `OptRe` provides about a 4dB improvement in SINR, which will improve network throughput significantly.

An illustrative example of transmitting a grayscale bitmap image via WARPs is provided in Fig. 13, demonstrating the effectiveness of `OptRe`. Without reflectors, the decoding error is too large to recognize the content of the graph due to the low SINR and RSS. Using reflectors at the Rx side, the decoding error is reduced. With `OptRe`, the decoding error is reduced further and we can easily identify the image as Starry Night by Vincent van Gogh.

4.3.4 *Impact of* `OptRe` *on Throughput*

To quantify the effect of `OptRe` on throughput, we built a test platform using 2 laptops with commodity WiFi cards as

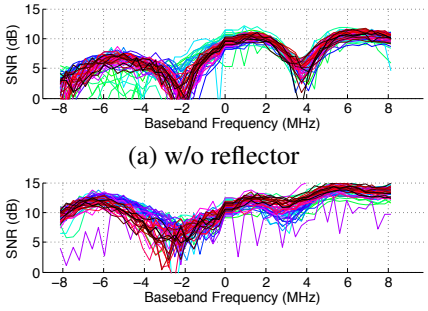

(a) w/o reflector

(b) `OptRe`

Figure 11: Performance of reflector in frequency.

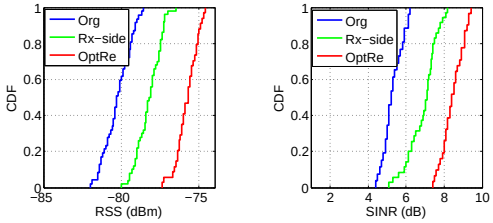

(a) CDF of RSS (b) CDF of SINR

Figure 12: RSS and SINR performance of reflectors.

Tx and Rx. We use iperf to transmit real-time TCP packets from Tx to Rx, and the bandwidth (or the maximum data rate) is set to 54Mbps. We conducted experiments in three target areas (orange areas *A*, *B* and *C* in Fig. 6(c)). Areas *A* and *B* represent typical office environments and area *C* for hallway layouts in office buildings. We randomly select 6 locations as training samples and apply our map generation — the accuracy of which has been verified in Section 4.2 — to predict the subareas having the lowest RSS.

Fig. 14 shows throughput in the three target areas. With reflectors at the Rx-side in A, the throughput was improved by 38%. Using `OptRe` in A, the throughput was 80% higher than the case of without reflectors, and 25% better than the case of placing reflectors at the Rx-side. Area B has simi-

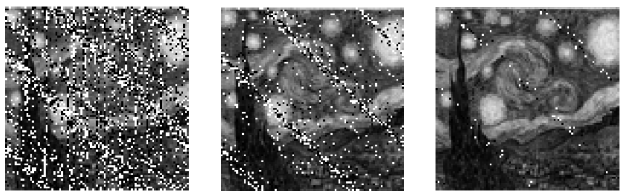

(a) w/o reflector (b) Rx side (b) `OptRe`

Figure 13: Image transmission result.

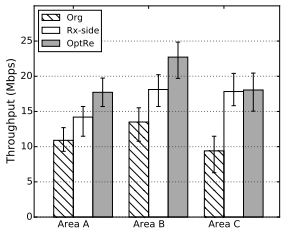

Figure 14: Throughput performance of reflectors.

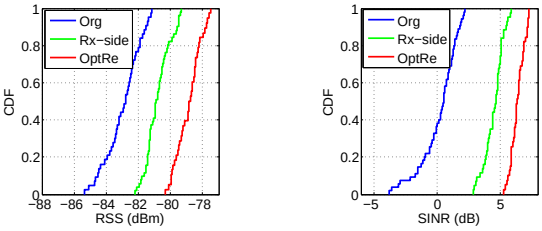

(a) CDF of RSS (b) CDF of SINR

Figure 15: RSS and SINR: Transmission power at 7dBm.

lar results as area A. In area C, the performance of OptRe is almost the same as placing reflectors at the Rx-side, both improving the throughput by around 90%. OptRe is no worse than reflectors at the Rx-side in all cases, and the reflectors at the Rx-side perform well as OptRe is placed only in the hallway with corner layouts.

5. USE-CASES

This section highlights OptRe in two use-cases: extension of the communication range of IoTs, and enhancement of security & privacy by customizing signal propagation.

Enhance coverage and connectivity: WiFi & IoTs

Section 4 has shown OptRe to improve the RSS, SINR and throughput of WiFi networks. Extending the range of IoT devices is challenging due to their limited power. OptRe suffices for IoT devices without requiring more advanced signal techniques or more power-efficient circuits. To evaluate a proof-of-concept of the capability of OptRe for IoTs, we use RSS and SINR as performance metrics. We set the transmission power of Tx/Rx WARP boards to 7dBm following the BLE standard [2] for IoT devices. Tx/Rx pair is placed in area *A* (Fig. 6(c)).

Fig. 15 shows the CDF distribution of RSS and SINR without reflectors, placing reflectors at Rx-side and using OptRe. Without reflectors, the RSS approaches the noise level. A negative SINR value means that the interference and noise are larger than the meaningful signal, thus making it impossible to decode. After placing reflectors at Rx-side, RSS was improved by 5dB and SINR by 90% to around 4dB. With OptRe, the SINR was improved further by 50% from 4dB to 6dB, compared to the case of placing reflectors at the Rx-side. This improvement of SINR allows Tx to use a higher modulation level, in order to increase network throughput. That is, OptRe not only improves the performance of WiFi networks, but also benefits IoT devices.

Customize signal propagation: security & privacy

Malicious users can eavesdrop transmission when the received signal is sufficiently strong. Even if users encrypt packets, they can get information such as AP beacons etc., which can be used to mount a denial of service (DoS) attack.

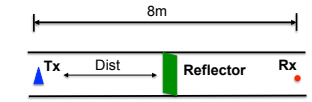

(a) Experiment Setup

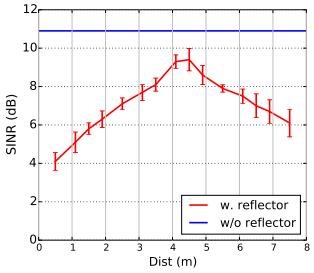

(b) SINR as the distance between Tx/reflector varies.

Figure 16: Proof-of-concept of security functions.

OptRe reflects signal with little loss, i.e., the signal can hardly penetrate through the metal reflectors. Therefore, it can restrict the signal within a trusted area, and prevents the sniffing attack in unexpected locations. Numerous researchers discussed defense mechanisms against DoS attack [22, 23], and sniffing attack [24, 25]. OptRe complements these existing schemes and provides physical-layer security. It depends on real scenarios to determine whether an area is trustable, which is part of our future work.

As a proof-of-concept of the potential use of OptRe for enhancing security, we compare SINR when the LOS path between Tx/Rx is blocked by a reflector and the case without reflectors. The distance between the Tx–Rx pair is set to 8m (Fig. 16(a)). We vary the distance between Tx/reflector, and Fig. 16(b) shows the results. The SINR is around 11dB without reflectors. After placing the reflector, SINR decreases. When the reflector is close to Tx, the SINR degrades by 63% to 4dB. SINR increases as the reflector moves away from the Tx, meaning that the signal blocking effect of reflectors decreases, and it attains the peak when the reflector reaches the middle between Tx/Rx. As the reflector further approaches Rx, SINR decreases. It requires a more sophisticated design for complete prevention of sniffing attack, and we only demonstrate the possibility by showing the effect of blocking LOS path between Tx and Rx. Note that the design of OptRe for the purpose of improving coverage (namely optimization module) can avoid the side-effect of the reflectors' ability to block signal by intelligent placement of reflectors.

6. DISCUSSION

Reflectors vs. Additional APs. Placing additional APs enhances network performance but causes additional cost and power consumption as well as mutual interference. Suppose OptRe increases the smallest SINR (and RSS) of Tx–Rx pairs using 802.11a by 4dB as shown in Section 4, then it increases the transmission range by 5m [26], which is 14%

greater than the typical 802.11a indoor transmission range of 35m [27], i.e., it requires 14% less APs and energy consumption. Since the exact number of APs will depend on the specific environment, we only provide a rough estimation. Considering a $350m \times 350m$ office, 100 enterprise APs are needed to cover the entire area, each of which costs about $400. With OptRe, 86 APs are enough to achieve a similar performance, reducing the cost of enterprise APs by $5,600. APs are also always on with a $6W$ power draw [28]. OptRe saves 756 $kW \cdot h$ power per year which equals about 358 kg of coal [29]. OptRe not only reduces the cost of APs and energy, but also eases the network maintenance.

Reflectors for Mobile Users. As long as users move around within the target area, OptRe can provide good performance.

Reflectors in a Multi-AP Environment Placement of reflectors for the case of multiple APs may use similar strategies as for the single AP scenario. The optimization module is the same as the single-AP case, and the map-generation module needs to be modified. In the single AP case, we add up multi-path signal strengths at Rx to estimate the RSS. Since different APs interfere with each other, the signals from APs other than the associated one degrade the desired signal. Instead of adding up all the signals to the Rx in the map-generation module, we subtract the strengths of signals from the other APs and only add the strengths of signals from the associated AP. The simulated annealing can also be applied to estimate the parameters, and we omit the details due to space limitation.

7. RELATED WORK

Wireless signal propagation models. Numerous efforts have been made to improve radio propagation models [11]. Helmholtz equation is used to model RF propagation as EM waves [30], but inverting the large sparse matrix in Helmholtz equation is computationally expensive and requires detailed information of the surrounding materials. An empirical propagation model was proposed in ARIADNE [13] using ray-tracing with limited training samples. However, this model requires re-measurements whenever reflectors are moved, making it impossible to use for reflector placement.

Studies about reflectors. Experiments were conducted after placing aluminum soda cans near routers in residential environments to enhance wireless signals [31]. Such experiments have shown a substantial bandwidth increase, but cannot provide any performance guarantees nor any scientific analysis. Wiprint [12] aimed to customize a wireless signal map using reflectors, but it required 3D printing to get the reflector which requires special and expensive equipment. In contrast, OptRe only uses cheap metal plates to enhance network performance.

8. CONCLUSION

In this paper, we have proposed OptRe which is the first analytical optimal placement of reflectors in an indoor environment and consists of map-generation and optimization modules. The simulation results match well with real-life measurements in both residential and office environments, validating the accuracy of map generation. Our experimental evaluation shows that the signal-map estimation error is within 4dB. We also evaluated the effect of reflector placement in OptRe, boosting the network throughput by up to 80%. We focused on the signle-AP case and briefly discussed its extension to the multiple-AP case. The detailed evaluation of the multiple-AP case is part of our future work.

Acknowledgement

The work reported in this paper was supported in part by the US NSF under Grant No. CNS-1317411.

9. REFERENCES

[1] FCC rules for unlicensed wireless devices work in ISM bands. http://www.afar.net/tutorials/fcc-rules.
[2] Bluetooth 4.0: Low energy. http://chapters.comsoc.org/vancouver/BTLER3.pdf.
[3] OFDM. https://en.wikipedia.org/wiki/Orthogonal_frequency-division_multiplexing.
[4] Beamforming. https://en.wikipedia.org/wiki/Beamforming.
[5] Rayleigh fading. https://en.wikipedia.org/wiki/Rayleigh_fading.
[6] H. Hashemi. The indoor radio propagation channel. *Proceedings of the IEEE*, 81(7):943–968, Jul 1993.
[7] D. Molkdar. Review on radio propagation into and within buildings. *IEEE Proceedings H - Microwaves, Antennas and Propagation*, 138(1):61–73, Feb 1991.
[8] T. S. Rappaport. Wireless communications: Principles and practice. prentice hall. *Prentice Hall*, 1996.
[9] A.Goldsmith. Wireless communications. *Cambridge University Press*, 2005.
[10] T. Chrysikos, G. Georgopoulos, and S. Kotsopoulos. Site-specific validation of itu indoor path loss model at 2.4 ghz. In *WoWMoM*. IEEE, 2009.
[11] Y. Zhang, C. Yin, C. Zheng, and K. Zhou. Computational hydrographic printing. *ACM Trans. Graph.*, 34(4), 2015.
[12] J. Chan, C. Zheng, and X. Zhou. 3d printing your wireless coverage. In *HotWireless*. ACM, 2015.
[13] Y. Ji, S. Biaz, S. Pandey, and P. Agrawal. Ariadne: A dynamic indoor signal map construction and localization system. In *MobiSys*. ACM, 2006.
[14] K. El-Kafrawy, M. Youssef, A. El-Keyi, and A. Naguib. Propagation modeling for accurate indoor wlan rss-based localization. In *Vehicular Technology Conference*. IEEE, 2010.
[15] Snell's Law. https://en.wikipedia.org/wiki/Snell%27s_law.
[16] LOS Propagation. https://en.wikipedia.org/wiki/Line-of-sight_propagation.
[17] C. R. Reeves, editor. *Modern Heuristic Techniques for Combinatorial Problems, Chapter 2*. John Wiley & Sons, Inc., 1993.
[18] Quickselect. https://en.wikipedia.org/wiki/Quickselect.
[19] Warp project. http://warpproject.org.
[20] Selective Channel fading. https://en.wikipedia.org/wiki/Fading.
[21] Wi-Fi SNR to MCS Data Rate Mapping Reference. http://www.revolutionwifi.net/revolutionwifi/2014/09/wi-fi-snr-to-mcs-data-rate-mapping.html.
[22] J. Mirkovic, S. Dietrich, D. Dittrich, and P. Reiher. *Internet Denial of Service: Attack and Defense Mechanisms (Radia Perlman Computer Networking and Security)*. Prentice Hall PTR, 2004.
[23] K. Y. Yau, C. S. Lui, F. Liang, and Y. Yam. Defending against distributed denial-of-service attacks with max-min fair server-centric router throttles. *Trans. Netw.*, 13(1), February 2005.

[24] L. Cai, S. Machiraju, and H. Chen. Defending against sensor-sniffing attacks on mobile phones. In *MobiHeld*. ACM, 2009.
[25] Y. Tung, S. Han, D. Chen, and K. G. Shin. Vulnerability and protection of channel state information in multiuser mimo networks. In *CCS*. ACM, 2014.
[26] S. Cebula, A. Ahmad, J. Graham, C. Hinds, L. Wahsheh, A. Williams, and S. DeLoatch. Empirical channel model for 2.4 ghz ieee 802.11 wlan. In *Conference on Wireless Networks*. Citeseer, 2011.
[27] How Far can a Wi-Fi Signal Travel:. `http://wifi.actiontec.com/learn-more/wifi-wireless-networking/how-far-can-a-wi-fi-signal-travel/`.
[28] Power Consumption of Enterprise AP. `https://dl.ubnt.com/datasheets/unifi/UniFi_AP_DS.pdf`.
[29] U.S. Energy Information Administration. `https://www.eia.gov/tools/faqs/faq.cfm?id=667&t=2`.
[30] Helmholtz equation. `https://en.wikipedia.org/wiki/Helmholtz_equation`.
[31] Dramatically improve wifi speed with a soda can! `https://www.youtube.com/watch?v=yz4aPaebe-k`.